



## Land Degradation, Desertification & Environmental Sensitivity to Climate Change in Alexandria and Beheira, Egypt



Mohamed E. Abou-Kota<sup>1</sup>, Hoda Hassaballa<sup>2</sup>, Maha Elhini<sup>2</sup>, and Shima K. Ganzour<sup>1\*</sup>

<sup>1</sup>Soils, Water and Environment Research Institute, ARC, Egypt

<sup>2</sup>The British University in Egypt, Department of Economics, Egypt

**L**AND degradation is one of the most important consequences of climate change that has socioeconomic repercussions world-wide, particularly in Egypt's Nile Delta region. It is therefore essential to inform of timely measurements of land degradation and identify its causes for the security of populations living on and near the Nile Delta. This paper calculates the Environmental Sensitivity Index using the MEDALUS-GEE (Mediterranean Desertification and Land Use in the Google Earth Engine) approach within two of Egypt's most climate-affected governorates, Alexandria and Beheira, on the district level. Results show that most of the districts in Alexandria is highly sensitive to climate change and is unsuitable for farming owing to their proximity to the Mediterranean Sea. The rise in sea level leads to the submergence of many lands. Besides, as a result of the geological composition of the region, seawater seeps into groundwater, all of which in turn was reflected in the rise in soil salinity. Also, the highest degree of land degradation and/or desertification was found in the hinterland of the Beheira Governorate, including high soil salinity and groundwater, which makes it difficult to undertake land reclamation and cultivation. Hence, the study suggests a crop suitability plan for the areas under study, particularly those highly subjected to land degradation and desertification.

**Keywords:** Land degradation, desertification, MEDALUS-GEE, Nile Delta, crop suitability.

### 1. Introduction

Arguably the most important environmental and socioeconomic issue today, particularly in Africa, is land degradation. The goal is for there to achieve no net land degradation on Earth by 2030. Also known as land degradation neutrality (LDN), by Sustainable Development Goal 15.3 (SDG 15.3). This goal is of high significance as it aims to conserve biodiversity and preserve ecosystems and lands (Prävālie et al., 2017). In 2019, the Intergovernmental Panel on Climate Change (IPCC) published a study on land degradation underlining the connection between land degradation and the extent and frequency of poverty among populations (Shukla et al., 2019). According to their report, the relation between land degradation and poverty becomes more pronounced as the

population grows, particularly in dry lands (UNCCD, 2017). Egypt, being characterized as dry and semi-dry, is currently experiencing several environmental stressors and extreme weather events including land degradation, the severity of which may lead to desertification. Such threats were expected to affect Egypt's agriculture sector and food security (Abdullahi et al., 2023). Egypt's Nile Delta is one of the world's most susceptible regions to climate change, as reported by the Intergovernmental Panel on Climate Change (IPCC, 2022). Saltwater intrusion into the Delta's groundwater has already raised salinization of the farmland, affecting agricultural output, and was expected to exert pressure on Egypt's food security (Amakrane et al., 2023). Such stressors have started to hit Egypt's agricultural production the hardest, given its vulnerability to climate change. Future projections highlight that sea

\*Corresponding author e-mail: sh.ganzour82@gmail.com

Received: 18/09/2023; Accepted: 17/11/2023

DOI: 10.21608/EJSS.2023.237386.1664

©2022 National Information and Documentation Center (NIDOC)

level rise (SLR) may flood vast areas of the coastal parts of the Nile Delta (Kulp & Strauss, 2019), flood large areas of agricultural land, as well as exposure of populations, property, infrastructure, and heritage to flooding (Vousdoukas *et al.*, 2022).

Desertification resulting from land degradation may threaten the welfare of millions of people in Egypt, particularly impoverished populations living in rural areas who make their living out of agricultural produce. The land was therefore considered a vital asset for urban and rural households' livelihoods, as it constitutes their primary source of food, energy, and shelter. The urge to rehabilitate degraded land and protect it from falling under the curse of desertification, helps vulnerable communities in fragile, resource-scarce environments to cope with shocks that are likely to jeopardize their existence. Hence, the novelty of this research attempts to gauge the recent level of desertification/land degradation in two of Egypt's Delta governorates, namely, Alexandria and Beheira on the district level; whereas, Alexandria, Egypt's largest coastal governorate and its second-largest city is encountering high climate change risk, namely sea level rise. Alexandria has 3283 persons per km<sup>2</sup>, forcing urban encroachment on agricultural lands. As well, Beheira is one of Egypt's largest Delta governorates that contributes to national agricultural production and is subject to soil salinization and desertification risk. Beheira has a high population density which corresponds to 987 persons per km<sup>2</sup>. Together, Alexandria and Beheira constitute 12.1% of Egypt's whole population (CAPMAS, 2022).

The appraisal of land degradation and/or desertification in Alexandria and Beheira was implemented via the calculation of the Environmental Sensitivity Index (ESI) using MEDALUS-GEE (Mediterranean Desertification and Land Use in the Google Earth Engine), which indicates the environmental sensitivity and variability to climate change in Alexandria and Beheira. Via this technique, it could be possible to find out the regions that are more subjected to desertification and influenced by land degradation therein. Moghanm and Belal (2018) and Elbasiouny (2018) carried out a similar study on an area in the north Nile Delta of Egypt. Also, Saleh *et al.* (2018) in the northern West Coast of Egypt.

Thus, the present study aims to assess land degradation and/or desertification in Alexandria and Beheira was implemented via the calculation of the Environmental Sensitivity Index (ESI) using MEDALUS-GEE.

## 2. Material and Methods

The study area included Alexandria and Beheira governorates (Figure 1).

### The Environmental Sensitivity Index

#### 2.1. Data

##### Soil

According to Hengl *et al.* (2017) the depth to bedrock (DBR), soil texture class (STC), soil organic matter (SOM), and drainage class (DC) were produced from the SoilGrids dataset with spatial resolution 250 m, which has been used in many similar studies (Elnashar, *et al.*, 2022, Fenta *et al.*, 2021 and Giuliani *et al.*, 2020). With a resolution of 5 arc-minutes, major soil groups (MSG) are plotted using the worldwide FGGD soils map (Van Velthuizen, 2007). The Global Vector Lithological Map (GLiM) database version 1.1 (Hartmann & Moosdorf, 2012) was used for the mapping of parent material (PM). Within the MEDALUS framework, FGGD and GLiM have been efficaciously deployed (Ferrara *et al.*, 2020). The soil quality index (SQI) was derived utilizing each of the aforementioned soil indicators.

##### Elevations

The near-global elevation data from the Shuttle Radar Topography Mission (SRTM) dataset was transferred at a 90-meter resolution (Jarvis *et al.*, 2008). In the GEE environment, slope and aspect were produced using SRTM (Gorelick *et al.*, 2017). Following other studies, Ferrara *et al.* (2020); Momirovi *et al.* (2019) and Morianou *et al.* (2021) the slope gradient (SG) was used in the SQI calculation, whilst the slope aspect (SA) was combined in the computation of the climatic quality index (CQI).

##### Vegetation

The surface reflectivity that was atmospherically corrected to account for water, clouds, heavy aerosols, and cloud shadows was used to calculate the Normalized Difference Vegetation Index (NDVI) (MOD13Q1 V6) (<https://doi.org/10.5067/MODIS/MOD13Q1.006>). Each month's highest value was used to produce the 16-day layers. Additionally, the yearly NDVI values were produced by taking the average value from the monthly layers. The vegetation quality index (VQI) employed by Ferrara *et al.* (2020) was calculated using the average NDVI from 2005 to 2020 for the production a plant cover mapping (PC).

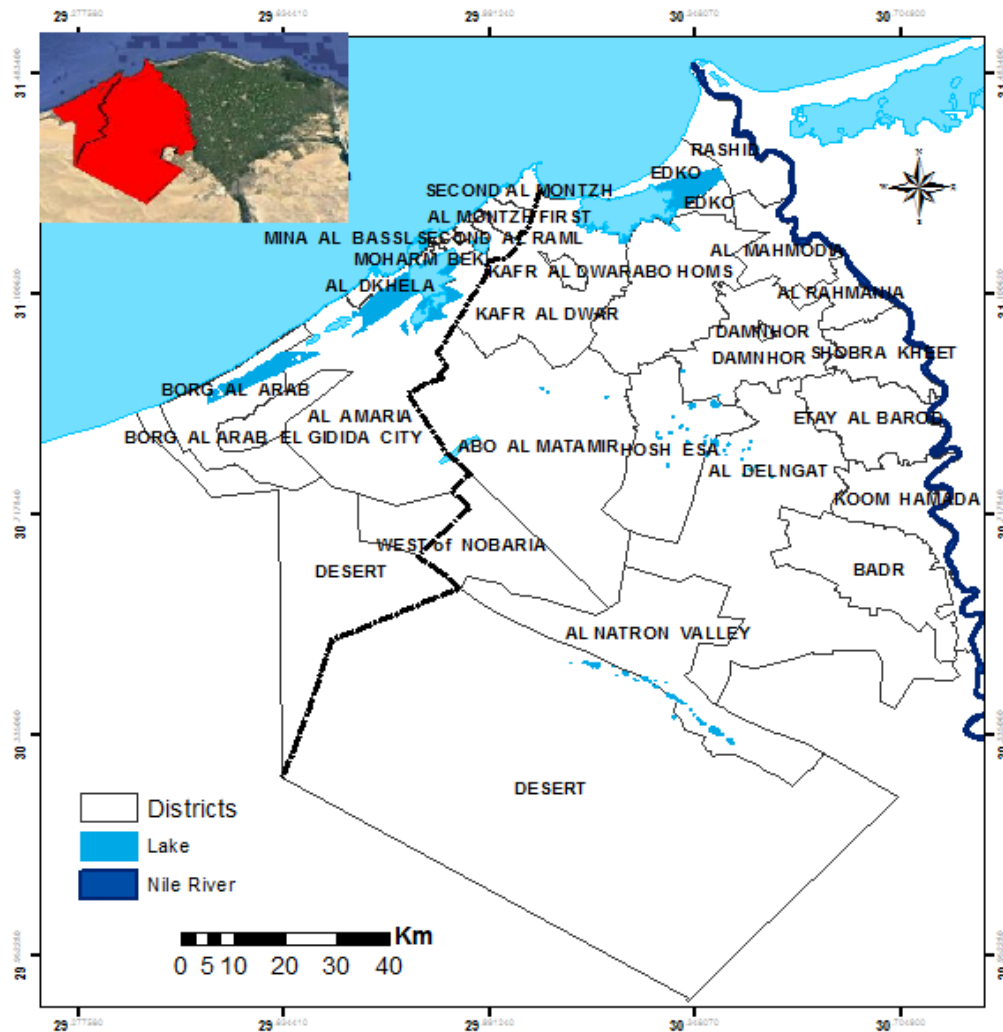


Fig. 1. Districts of study area.

### Land cover

The information on land cover was derived from the Climate Change Initiative Land Cover (ESA; CCILC) of the European Space Agency (ESA) from 1992 to 2020 (Bontemps et al., 2012; ESA, 2015 and ESA, 2018), later Land Use Land Cover (LULC) it has been effectively used in the MEDALUS framework and is available at 300 grids (Ferrara et al., 2020). Through their mode, the yearly layers from 2005 to 2020 were integrated into a single layer. Ferrara et al. (2020) used the latter to map land use intensity (LUI) for the management quality index (MQI) computation as well as fire risk (FR), drought resistance (DR), and erosion prevention (EP).

### Precipitation

The daily  $0.05^\circ \times 0.05^\circ$  grid from the Climate Hazards Group Infrared Precipitation with Station data (CHIRPS) dates back to 1981 (Funk et al., 2015). Besides having reasonably high geographical and temporal resolution and long-term data

availability, compared to previous East African rainfall goods, this dataset fared best. (McNamara et al., 2021). The total number of pentad layers for every month was used to construct monthly rainfall layers, and the total number of months for the year was used to obtain yearly rainfall values. For the CQI calculations, the average rainfall (P) rate from 2005 to 2020 was utilized (Lahloui et al., 2017). To calculate the adjusted Fournier Index (Arnoldus, 1977) as an indicator of rainfall erosivity, the average monthly P value from January to December was combined with the annual layer (De Pina Tavares et al., 2015).

### Evapotranspiration

The synthetic ET at 1 km was the ET dataset used for the research area (Elnashar et al., 2021a). To minimize uncertainty related to their techniques, entries, and variables, this dataset was made using the simple mean of the Penman-Monteith-Leuning (Zhang et al., 2019) and the functioning Simplified Surface Energy Balance (Senay et al., 2013). The aggregate of all the months in each year was used to

create the annual ET values. For the CQI calculation, the mean ET value from 2005 to 2020 was employed (Afzali *et al.*, 2021 and Lahlaoui *et al.*, 2017).

### 2.1.1 Ancillary data sources

WorldClim global climate data (Trabucco and Zomer, 2018) provided the mean worldwide aridity index (AI) at 1 km. This data was used to calculate the CQI (Momirovi *et al.*, 2019). The global Gridded Population of the World version 4 (GPWv4) at 30 arc-second resolution was used to map population density (PD) (CIESIN, 2018). By calculating the mean (average), the current research combined the 4 population layers from 2005, 2010, 2015, and 2020 to a single layer. For MQI calculation, the last layer was used (Ferrara *et al.*, 2020). Elnashar *et al.* (2021b) acquired data on water erosion (WE) from the papers, which they then used to calculate the SQI (Afzali *et al.*, 2021).

### 2.2 Calculations

The vulnerable areas to desertification and its motives inside qualitative, quantitative, and spatial must be thoroughly understood in order to analyse the productivity of degraded land. SQI, CQI, VQI, and MQI are the four sub-indices that make up the ESI, which is the environmentally sensitive indicator to desertification (Wijitkosum, 2021). In order to match the LULC layer's spatial resolution, ESI was produced at 300 m grids. The temporal, and spatial datasets needed for this investigation are taken from a variety of sources, a synopsis of which was included in the paper have Elnashar, *et al.* (2022), to the updated information supplied in the GEE (Table 1), we used the broadest indices and their relatively sensitivity scores (RSS) to land degradation which has been widely utilized on a worldwide scale (Tables 2–5). The next subsections show each quality indicator together with the ESI index to desertification those results.

#### \* SQI

By the geometric mean (GM) of the relatively sensitivity scores ( $R_s$ ) of 8 soil indicators, Table 2, and Equ. 1, the SQI in the MEDALUS-GEE was established.

$$SQI = (STC_s, SOM_s, DBR_s, MSG_s, SG_s, WE_s, PM_s, DC_s)^{1/8}$$

Equ. (1)

$STC_s$ ; sensitivity score for texture class of soil,  $SOM_s$ ; sensitivity score for organic matter of soil,  $DBR_s$ ; sensitivity score for depth to bedrock,  $MSG_s$ ; sensitivity score for major soil group,  $SG_s$ ; sensitivity score for slope gradient,  $WE_s$ ; sensitivity score for water erosion,  $PM_s$ ; sensitivity score for parent material, and  $DC_s$ ; sensitivity score for the drainage class.

#### \* CQI

Climate indications clarify how climate affects rainfall aggressivity, the impact of microclimates, and water availability to agroecosystems. The GM of the  $R_s$  of 5 climatic indicators, Table 3, and Equ. 2, were used to determine CQI in current MEDALUS-GEE.

$$CQI = (SA_s, AI_s, E_s, ET_s, P_s)^{1/5}$$

Equ. (2)

$SA_s$ ; sensitivity score for slope aspect,  $AI_s$ ; sensitivity score for the aridity index,  $E_s$ ; sensitivity score for rainfall erosivity through MFI,  $ET_s$ ; sensitivity score for evapotranspiration,  $P_s$ ; sensitivity score for rainfall.

#### \* VQI

Indicators of vegetation reveal motives that vegetation counteracts the consequences of deterioration and desertification. To be more precise, plant cover describes motives that vegetation decreases runoff & sediment loss, dryness resistance describes motives that vegetation copes with extreme dryness, fire risk describes motives that vegetation manages fires, and preventing erosion describes motives that vegetation avoids soil erosion. Utilizing Table 4, Equ. 3, and the GM of the  $R_s$  of 4 vegetation indicators, the current MEDALUS-GEE calculates the VQI.

$$VQI = (DR_s, PC_s, EP_s, FR_s)^{1/4}$$

Equ. (3)

$DR_s$ ; sensitivity score for the drought resistance,  $PC_s$ ; sensitivity score for plant cover,  $EP_s$ ; sensitivity score for erosion protection, and  $FR_s$ ; sensitivity score for the fire risk.

#### \* MQI

The phenomenon of desertification and degradation was accelerated or prevented by human activity, according to management indicators, Equ. 4 and Table 5, GM of the  $R_s$  of 2 management indicators, the MQI, were used to generate MQI in current MEDALUS-GEE.

$$MQI = (PD_s, LUI_s)^{1/2}$$

Equ. (4)

$PD_s$ ; sensitivity score for the population density, and  $LUI_s$ ; sensitivity score for the land use intensity.

#### \* ESI

According to the GM of 4 quality metrics, Equ. 5, Table 6 and figure 2 the MEDALUS framework classifies sensitive areas endangered via desertification.

$$ESI_i = (SQI_i, CQI_i, VQI_i, MQI_i)^{1/4}$$

Equ. (5)

**Table 1. Data description and sources for the MEDALUS-GEE.**

Index	Indicator	Dataset	Resolution	Source
SQI	STC	Soil Grids	250m	earth engine
	SOM	Soil Grids	250m	
	DBR	Soil Grids	250m	isric.org
	MSG	FGGD	10km	
	SG	SRTM	90m	earth engine
	WE	RUSLE-GEE	90m	doi.org
	PM	GLiM	vector	ccgm.org
CQI	DC	Soil Grids	250m	earth engine
	SA	SRTM	90m	cgiarcsi.community
	AI	CGIARCSI	1km	
	E	CHIRPS	5km	
	ET	Synthesized ET	1km	
P	CHIRPS	5km		
VQI	PC	NDVI	250 m	earth engine
	DR	LULC	300m	maps.elie.ucl.ac.be
	EP	LULC	300m	
FR	LULC	300m		
MQI	PD	GPWv411	1km	earth engine
	LUI	LULC	300m	maps.elie.ucl.ac.be

**Table 2. Soil quality index (SQI) indicators, their range/classes, and relative sensitivity scores in MEDALUS-GEE.**

Indicators	Range/Class	Scores	Key references
Soil Texture Class (STC)	Sa	2.00	(Budak et al., 2018; Ferrara et al., 2020; Lahloai et al., 2017 and Momirović et al., 2019)
	Si; Cl; SiCl	1.60	
	SaCl; SiLo; SiClLo	1.20	
	Lo; SaClLo; SaLo; LoSa; ClLo	1.00	
Soil Organic Matter (SOM %)	<1	2.00	(Budak et al., 2018; De Pina Tavares et al., 2015; Kosmas et al., 2014 and Momirović et al., 2019)
	1 – 2	1.70	
	2 – 3	1.50	
	3 – 6	1.20	
	>6	1.00	
Depth to Bedrock (DBR) (cm)	<15	2.00	(De Pina Tavares et al., 2015; Kosmas et al., 2014 and Momirović et al., 2019)
	15 – 30	1.80	
	30 – 60	1.60	
	60 – 100	1.40	
	100 – 150	1.20	
Major Soil Group (MSG)	>150	1.00	(Ferrara et al., 2020 and Van Velthuizen, 2007)
	GY; LP; SC; SN; RK; DS; TS	2.00	
	AR; RT	1.70	
	CL	1.60	
	AL; LX; PD; PL	1.50	
	AC; AT; FR; GL; LV;PZ; RG; VR	1.30	
	GR; KS; NT; PH	1.10	
AN; CH; CM; FL; HS	1.00		
Slope Gradient (SG%)	>36	2.00	(Budak et al., 2018; De Pina Tavares et al., 2015; Ferrara et al., 2020; Kosmas et al., 2014 and Momirović et al., 2019)
	30 – 36	1.70	
	24 – 30	1.50	
	18 – 24	1.50	
	12 – 18	1.30	
	6 – 12	1.20	
	3 – 6	1.10	
Water Erosion (WE) (t ha <sup>-1</sup> yr <sup>-1</sup> )	<3	1.00	(Afzali et al., 2021; Kosmas et al., 2014; Symeonakis & Drake, 2004 and Wijitkosum, 2021)
	>50	2.00	
	30 – 50	1.70	
	15 – 30	1.50	
	5 – 15	1.20	
Parent Material (PM)	<5	1.00	(Budak et al., 2018 and Ferrara et al., 2020)
	PY	2.00	
	SC	1.70	
	PA; VA	1.60	
	VI; PI; MT	1.50	
	SM	1.40	
	VB; SS; PB; EV	1.20	
	SU	1.00	
P; VP; E	2.00		
Drainage Class (DC)	SM	1.70	(Boudjemline & Semar, 2018 and Ferrara et al., 2020)
	I	1.40	
	MW	1.20	
	M	1.00	

Cl; clay, Sa; sand, Si; silt, Lo; loam, GY; Gypsysol, LP; Leptosol, SC; Solonchaks, SN; Solonetz, RK; Rock debris, DS; Sand dunes, TS; Salt flats, AR, Arenosol; RT; Plinthosol, CL; Calcisol, AL; Alisol, LX; Lixisol, PD; Podzoluvisol, PL; Planosol, AC; Acrisol, AT; Anthroso, FR; Ferrasol, GL; Gleysol, LV; Luvisol, PZ; Podzol, RG; Regosol, VR; Vertisol, GR; Greyzem, KS; Kastanozem, NT; Nitisol, PH; Phaenozem, AN; Andosol, CH; Chernozem, CM; Cambisol, FL; Fluvisol, HS; Histosol, PY; Pyroclastics, SC; Carbonate sedimentary rocks, PA; Acid plutonic rocks, VA; Acid volcanic rocks, VI; Intermediate volcanic rocks, PI; Intermediate plutonic rocks, MT; Metamorphic rocks, SM; Mixed sedimentary rocks, VB; Basic volcanic rocks, SS; Siliciclastic sedimentary rocks, PB; Basic plutonic rocks, EV; Evaporites, SU; Unconsolidated sediments, P, Poor, PV; Very poor, E, excessive, I, Imperfectly, MW; Moderately well, W; Well.

**Table 3. Climate quality index (CQI) indicators, their range/classes, and relative sensitivity scores in MEDALUS-GEE.**

Indicators	Range/Class	Scores	Key references
Slope Aspect (SA)	S; SW; SE; E	2.00	(Ait Lamqadem et al., 2018; De Pina Tavares et al., 2015; Kosmas et al., 2014; Momirović et al., 2019; Morianou et al., 2021)
	N; NW; NE; W	1.00	
	< 0.03	2.00	
	0.03 – 0.10	1.75	
	0.10 – 0.20	1.55	
Aridity Index (AI)	0.20 – 0.35	1.45	(Boudjemline & Semar, 2018; Lahlaoui et al., 2017 and Momirović et al., 2019)
	0.35 – 0.50	1.35	
	0.50 – 0.65	1.25	
	0.65 – 0.75	1.15	
	0.75 – 1.00	1.05	
	> 1.00	1.00	
	>200	2.00	
Erosivity (E; driven from Modified Fournier Index.)	150 – 200	1.70	(De Pina Tavares et al., 2015 and Momirović et al., 2019)
	100 – 150	1.50	
	50 – 100	1.20	
	<50	1.00	
	>1600	2.00	
	1400 – 1600	1.80	
Evapotranspiration (ET, mm yr <sup>-1</sup> )	1200 – 1400	1.65	(Afzali et al., 2021; Jafari et al., 2016; Lahlaoui et al., 2017 and Sepehr et al., 2007)
	1000 – 1200	1.50	
	800 – 1000	1.35	
	600 – 800	1.25	
	400 – 600	1.15	
	200 – 400	1.05	
	<200	1.00	
	<200	2.00	
	200 – 400	1.80	
	400 – 600	1.65	
Rainfall (P, mm yr <sup>-1</sup> )	600 – 800	1.50	(Ferrara et al., 2020 and Lahlaoui et al., 2017)
	800 – 1000	1.35	
	1000 – 1200	1.25	
	1200 – 1400	1.15	
	1400 – 1600	1.05	
	>1600	1.00	

S: South; N: North; W: West; E: East.

**Table 4. Vegetation quality index (VQI) indicators, their range/classes, and relative sensitivity scores in MEDALUS-GEE.**

Indicators	Range/Class	Scores	Key references
Drought Resistance (DR; driven from LULC)	200;201;202	2.00	(Ferrara et al., 2020; Lahlaoui et al., 2017 and Momirović et al., 2019)
	11;130;150;153	1.60	
	10;30;40;120;151;152	1.50	
	20;100;122	1.40	
	12;81;82;110	1.30	
	62;72;80;121	1.20	
	60;70;71;180	1.10	
	50;61;90;140;160;170	1.00	
	<0.10	2.00	
	0.10 – 0.11	1.90	
Plant Cover (PC; driven from NDVI)	0.11 – 0.13	1.80	(Ferrara et al., 2020 and Lahlaoui et al., 2017)
	0.13 – 0.18	1.70	
	0.18 – 0.26	1.60	
	0.26 – 0.38	1.50	
	0.38 – 0.50	1.40	
	0.50 – 0.62	1.30	
	0.62 – 0.72	1.20	
	0.72 – 0.80	1.10	
>0.80	1.00		
Erosion Protection (EP; driven from LULC)	200; 201;202	2.00	(Ferrara et al., 2020; Lahlaoui et al., 2017 and Momirović et al., 2019)
	11	1.80	
	10;150;153	1.70	
	12;120;122;151;152	1.60	
	30;81;82	1.50	
	20;40;62;130	1.40	
	72;80;110	1.30	
	100;121;170;180	1.20	
	60;70;140	1.10	
	50;61;71;90;160	1.00	
62	1.70		
Fire Risk (FR; driven from LULC)	121	1.60	(Ferrara et al., 2020 and Lahlaoui et al., 2017)
	30;70;100	1.50	
	10;11;20; 40;60;110;120;122	1.40	
	50;61;71;80;81;82;130;150;153	1.30	
	12; 72;151;152	1.20	
	90;170;180	1.10	
140;160;200;201;202	1.00		

LULC; Land Use Land Cover and NDVI; Normalized Difference Vegetation Index.

**Table 5. Management quality index (MQI) indicators, their range/classes, and relative sensitivity scores in MEDALUS-GEE.**

Indicators	Range/Class	Scores	Key references
Population Density (PD, person km <sup>-2</sup> )	>2700	2.00	(Budak et al., 2018 and Ferrara et al., 2020)
	2000 – 2700	1.90	
	1400 – 2000	1.80	
	850 – 1400	1.70	
	500 – 850	1.60	
	300 – 500	1.50	
	170 – 300	1.40	
	80 – 170	1.30	
	30 – 80	1.20	
	4 – 30	1.10	
Land Use Intensity (LUI; driven from LULC)	<4	1.00	(Ferrara et al., 2020; Lahloai et al., 2017 and Momirović et al., 2019)
	200; 201;202	2.00	
	150	1.80	
	10;11120;153	1.70	
	20;122;151;152	1.60	
	30;40;81;82;110;121;130	1.50	
	12	1.40	
	62;160;180	1.30	
	60;72;100;140;170	1.20	
	50;70;71;80	1.10	
61;90	1.00		

**Table 6. Quality indices and the resulting ESI, their range, and description in MEDALUS-GEE.**

Index	Range: Description	Key references
SQI	1.00 – 1.13: HQ	(Boudjemline & Semar, 2018 and Ferrara et al., 2020)
	1.13 – 1.45: MQ	
	>1.45: LQ	
CQI	1.00 – 1.20: HQ	(Ferrara et al., 2020)
	1.20 – 1.50: MQ	
	>1.50: LQ	
VQI	1.00 – 1.13: HQ	(Ferrara et al., 2020)
	1.13 – 1.38: MQ	
	>1.38: LQ	
MQI	1.00 – 1.30: HQ	(Bedoui, 2020 and Ferrara et al., 2020)
	1.30 – 1.50: MQ	
	>1.50: LQ	
ESI	1.000 – 1.170: NAA (VLSL)	(Ferrara et al., 2020 and Momirović et al., 2019)
	1.170 – 1.225: PAA (LSL)	
	1.225 – 1.275: FAA1 (MSL)	
	1.275 – 1.325: FAA2 (MSL)	
	1.325 – 1.375: FAA3 (MSL)	
	1.375 – 1.425: CAA1 (HSL)	
	1.425 – 1.530: CAA2 (HSL)	
>1.530: CAA3 (HSL)		

LQ; Low Quality, MQ; Moderate Quality, HQ; High Quality, AA; Affected Area, N; Not, P; Potentially, F; Fragile, C; Critically, SL; Sensitivity Level, V; Very, L; Low, M; Medium, H; High.

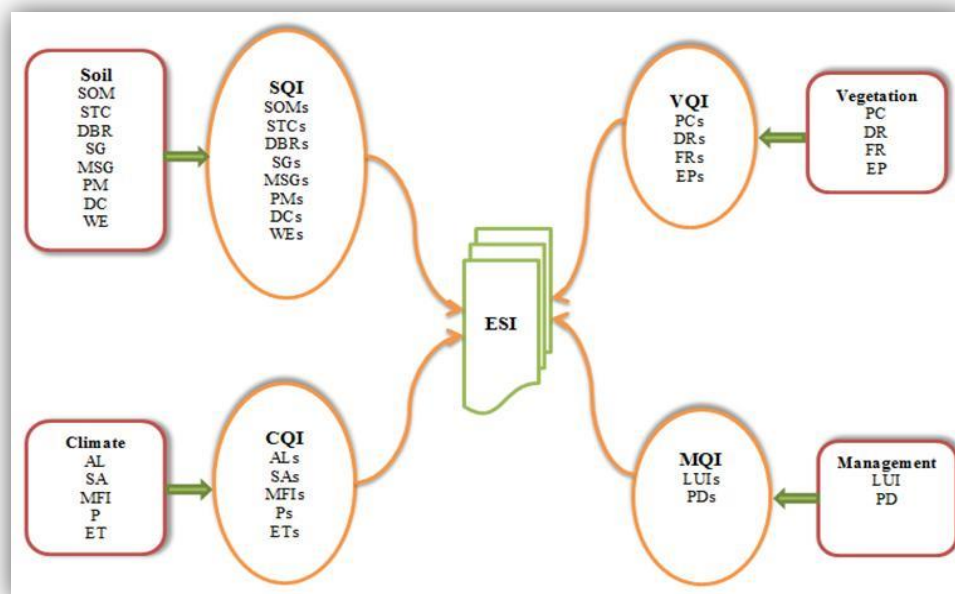


**Fig. 2. Flowchart of the framework of the study.**

### 3. Results

The findings of the ESI estimates indicating the various degrees of climate change sensitivity in Alexandria and Beheira. Generally, each of the four quality index sub-indicators (SQI; CQI; VQI; & MQI) has 3 separate valuation ranges (high; moderate; & low), and there are 4 kinds of land services (sensitivity level) with 8 sub-levels for each (Review Table 6), a favorable balance between natural and anthropogenic influences may be seen in the first group, which is made up of areas that were not affected by land degradation (not affected area or NAA). The second category, known as a potentially affected area (PAA), includes places that are particularly susceptible to land degradation in the event of any significant anthropogenic or natural change. The third classification designates regions that should be subject to land conservation measures to stop desertification since even a little shift in the relative importance of anthropogenic and natural activities is likely to cause land degradation processes. These areas are known as fragile affected areas or FAAs. The fourth category, known as a critically affected area (CAA), displays places that have already seen severe degradation and are on the verge of becoming decertified. In order to stop desertification, these places need to be subject to immediate land conservation efforts.

#### 3.1. SQI

Map 1 below shows the SQI, the ability of the soil to hold water and its natural resistance to erosion processes are both impacted by soil markers of land degradation. Most SQI lies between low to moderate quality. Even within the eastern part of the investigated areas which have the most fertile land because this part is adjacent to the Nile branch, is also scattered with moderate-quality soil. This is probably due to the high hazards of alkalinity and salinity of the soil, which are considered the most ecological risks, threaten the quality of the soil. The alkalization degree in Beheira and Alexandria is very high as their pH was found to be almost 8.5. In addition, both governorates have relatively low slopes compared to the rest of Egypt, thereby salts are excessively released, transported, and concentrated on their topsoil, especially in the Noubaria district. The lowest slope in Alexandria is specifically threatened by an extreme climatic event which is the sea level rise (SLR). The increase in SLR intensifies the degree of salinity in the soil, affecting the underground water resources and accelerating the erosion of the infrastructure. Therefore, climatic change along with natural

occurrences affects the soil's quality, negatively affecting the vegetation quality.

#### 3.2. CQI

Map 2 below shows the climate quality index (CQI). It indicates that the studied area was commanded by a low climate quality index (CQI >1.5; LQ). The arid climate conditions along with the rising increases in the temperature of the soil followed by high evapotranspiration rates influence the composition of the fertile land foundations. Additionally, the changes in climatic conditions affect the availability of water to the soil which inhibits its productivity and contributes further to reducing the quality of the climate, which in turn increases vulnerability to land degradation and desertification.

#### 3.3. VQI

Map 3 below shows the VQI, it indicates that the North-eastern part was classified as medium quality (VQI<1.38), while the western and southern portions of the studied area were characterized by its low-quality (VQI>1.38) which could be attributed to low water resources and desert conditions. The repercussions of climate change, which are represented by increased soil salinity, soil dryness, and increased soil temperature, have led to the lack of conditions suitable for the normal growth rate of the plant, thus a decrease in the plant density index and a lower plant cover. Therefore, since crops in Egypt have a low NDVI, this puts severe pressure on the Egyptian food security dilemma.

#### 3.4. MQI

Map 4 below shows MQI which depicts the human constituent (compression of human activity) on the environment. The majority of the study area was mapped as low managed (LQ) where the management quality index is higher than 1.50 mainly around the Nile branch but the rest of the studied area was dominated by a medium MQI (1.30-1.50) and the minority was clustered as high MQI (<1.30). MQI consists of sub-indices that accelerate the deterioration of the Egyptian fertile land, namely, population density and land use intensity. Other adverse anthropological activities include over-irrigation, inefficient use of heavy machines, lack of suitable technological machines, excessive application of harmful chemical fertilizers that led to unprecedented pressure on Egyptian agricultural land, pollution, waste discharged from factories, and sewage water flowing into the Mediterranean coastal region. These factors have both direct and direct effects on desertification.

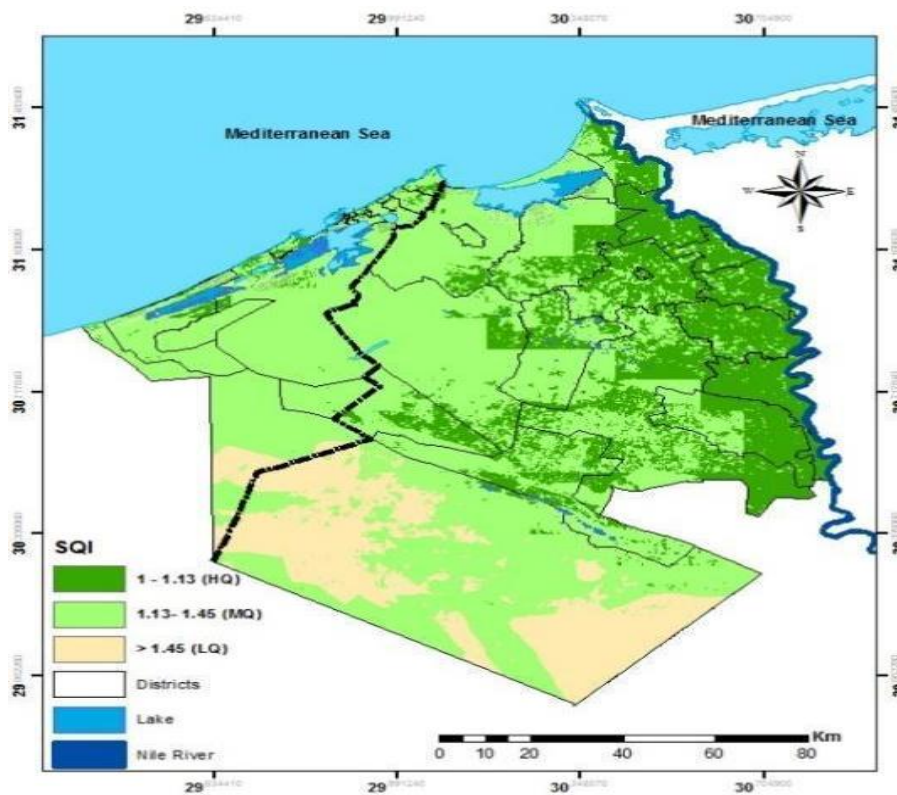
### 3.5. ESI

The (aggregated) environmental sensitivity index (ESI) is shown in Map 5 below. It indicates that the study area is under medium to high sensitivity levels, but most of the area was clustered as highly sensitive to land degradation ( $ESI > 1.375$ ). Changes in climatic factors, coupled with a high degree of salinity and inefficient human activities led to high sensitivity to land degradation. At the current alarming rate of land misuse, the fertile land in the Delta region is in jeopardy and at a high risk of desertification in the forthcoming years.

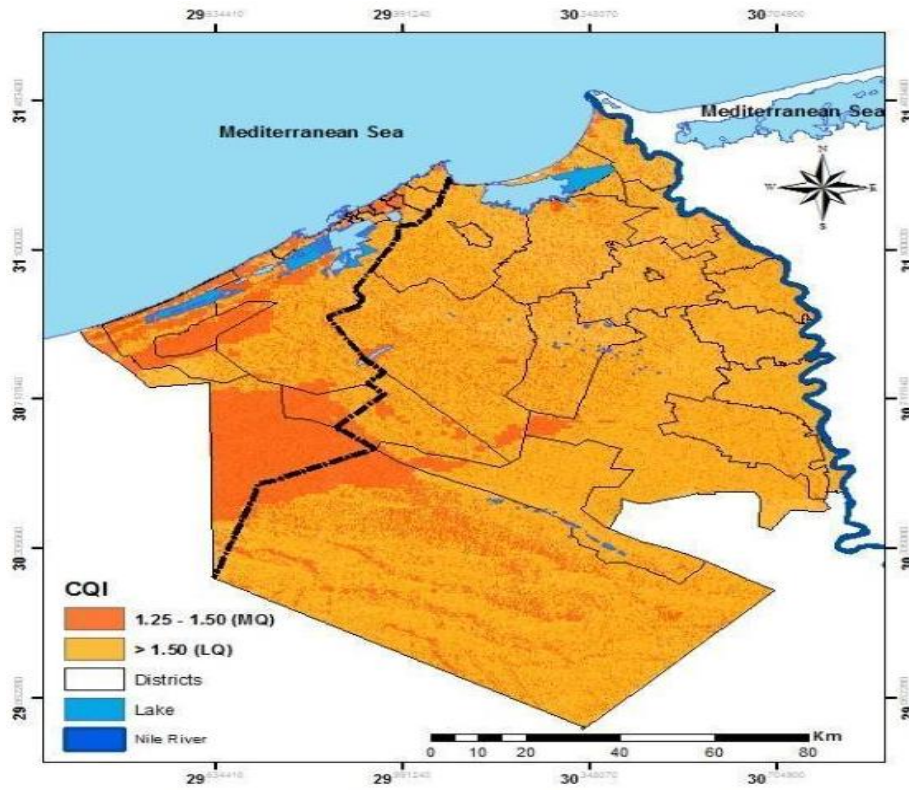
### 4. Discussion

The maps 1:5 and Figure 1 indicates that most of the districts in Alexandria, as they appear on map 5, are unsuitable for farming owing to their proximity to the Mediterranean Sea, adding to that industrial activity located there. The highest degree of land degradation and desertification ( $> 1.530$ : CAA3 (HSL)) was concentrated in the Beheira Governorate, specifically the Qattara Depression area and Wadi Al-Maghra (representing 46% of the total area of the hinterland of the Beheira Governorate). Reasons beyond increasing degradation in this area could be high soil salinity,

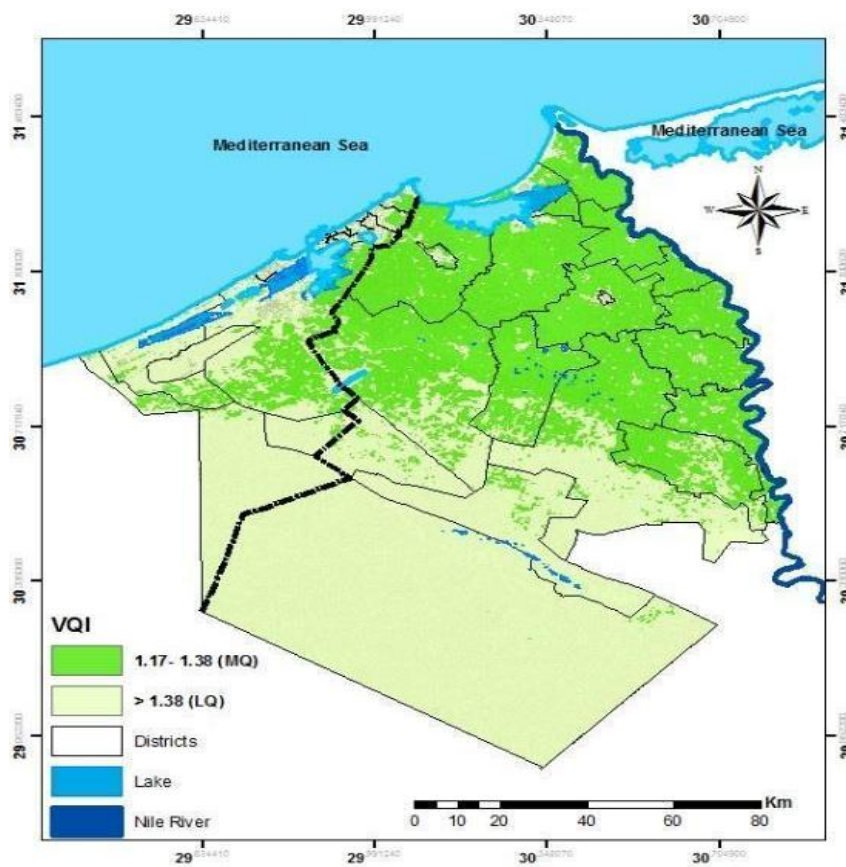
the rise in the sea level, which was reflected in the groundwater, as well as the geological composition of the region, is raising soil salinization as well as the content of calcium carbonate ( $\text{CaCO}_3$ ). Also, parts of the Beheira governorate located in the area surrounding Lake Edku (the northern part of the district of Edku and Abu Homs), were affected by soil salinity, making it impossible to be cultivated. Therefore, it is preferable to modify the region's strategy, by converting land use therein towards fish farming (aquaculture) rather than agriculture. Fish farming is a stage of plant culture that was confirmed by the General Authority for Construction Projects and Agricultural Development affiliated with the Ministry of Agriculture and Land Reclamation. The southern part of Beheira, in the Edko district, has a degradation level of (1.425 – 1.530: CAA2 (HSL)). The hinterland desert of the Beheira governorate, in addition to the southwestern part of the districts of Dalangat, western Nubariya, and Wadi el-Natron, are the effect of the lack of soil nutrient availability, in addition to the failure of improving their nutritional status via adding soil conditioners, because of their high content of calcium carbonate, which immobilize these nutrients in soil (Nada et al., 2023).



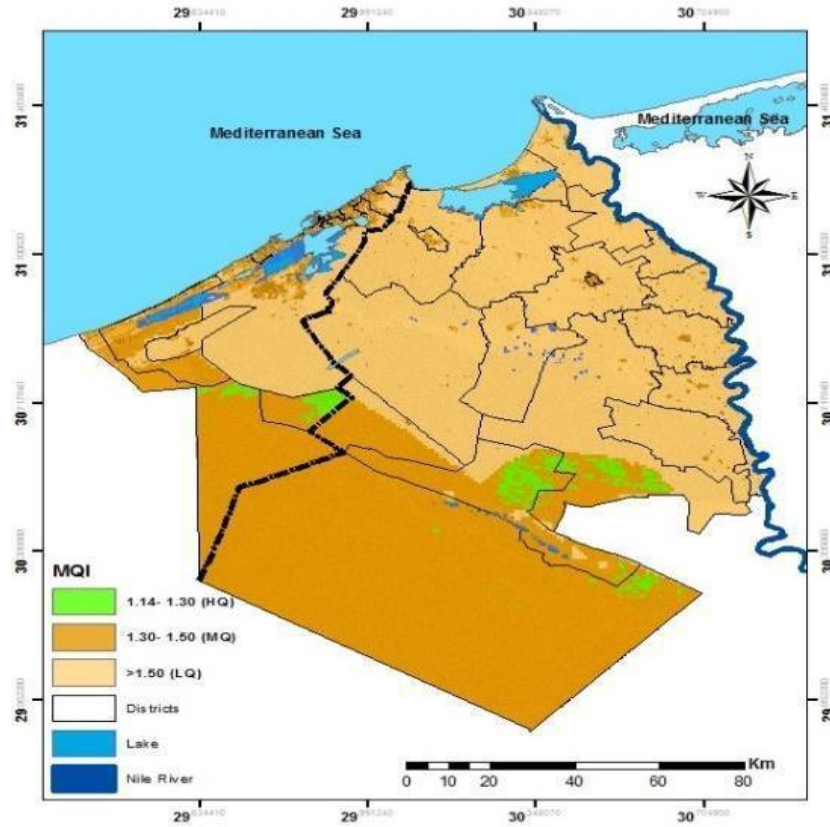
Map 1. Soil Quality Index (SQI).



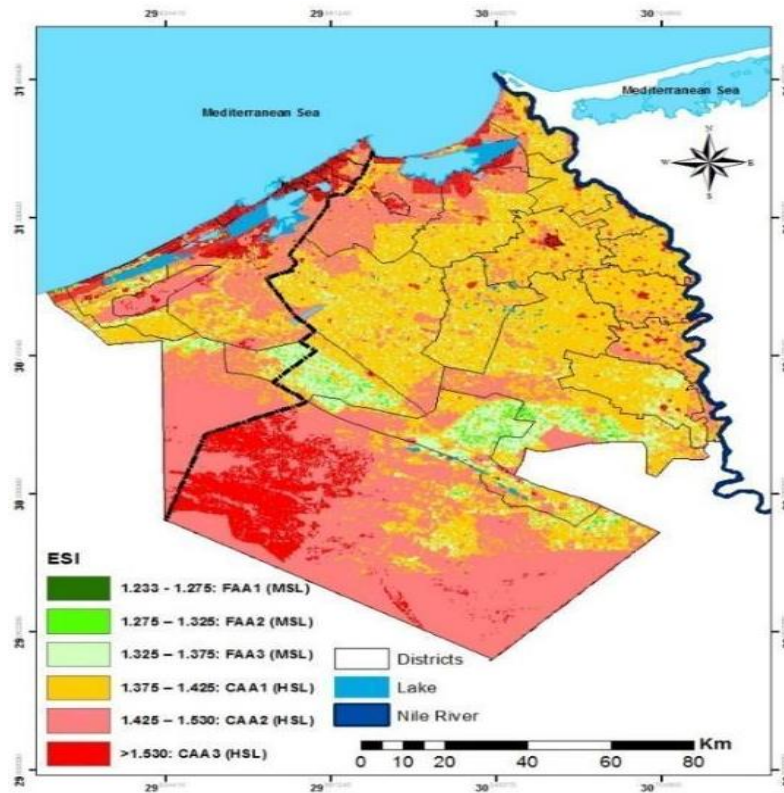
Map 2. Climate Quality Index (CQI).



Map 3. Vegetation Quality Index (VQI).



Map 4. Management Quality Index (MQI).



Map 5. Environmental Sensitivity Index (ESI).

The areas of the governorates of Behira and Alexandria that are at (1.375 – 1.425: CAA1

(HSL)) represent 40.89 percent of the total study area. This area includes the districts (Rashid, Al-

Mahmudiyah, Al-Rahmaniyah, Shubrakhit, Itay El-Baroud, Kom Hamada, Badr, Al-Dalanjat, Damanhour, Abu Homs, Hosh Essa, Abu El-Matamir). Alexandria includes districts (southwest of the modern city of Burj Al Arab, which is a potential area for land reclamation which includes the agricultural greenhouses of the Muhammad Naguib military base). This degree was considered a watershed, and its further deterioration will be a disaster for Egypt's agricultural production. Relevant policies include:

1. Promote spatial applications and models for early warning signs of land degradation and desertification problems.
2. Develop a prevention and mitigation strategy by adopting agricultural technologies and practices linked to sustainable and integrated management in the long term.
3. Implement rationing to the utilization of chemical fertilizers and initiate the trend towards the use of bio-fertilizers.
4. Establish associations for small farmers to transfer the most important recommendations of applied research.

The recommendation for the crop composition of this region was based on the physicochemical properties and soil content of elements, in addition to climate factors, on top of which are temperature and relative humidity. Suggested crops include summer rice, municipal beans, maize, flax, barley, sunflowers, soybeans, sustainable alfalfa, sugar beet, peanuts, wheat and cotton, and sesame. These crops achieve a substantial profit margin, in addition to raising the economic efficiency of using the water resources to reduce the wasteful use of irrigation water.

The central Delta region, close to Gharbia Governorate, at (1.325 – 1.375: FAA3 (MSL)) was epitomized in limited parts in the districts of West Nubaria, Wadi El-Natrun, and Badr. This level represents 11.94 percent of the total studied and cultivated area in the targeted study area. The same regions and a small part in the northwestern side of Burj Al-Arab in Alexandria Governorate contain another degree (1.275 – 1.325: FAA2 (MSL)) and represent 1.28 percent of the total studied cultivated area in the target study area. There is also a degree (1.225 – 1.275: FAA1 (MSL)) that represents 0.04 percent of the total studied and cultivated area in the targeted study area and it was concentrated in three districts only in El-Beheira governorate, which are west of Nubariya, Wadi El-Natrun, and Badr. Knowing that the classification of the three degrees as mentioned earlier is medium deterioration because of poor soil fertility index (SFI), fragmentation of agricultural holdings, and failure to follow a unified agricultural cycle create environmental problems that increase their vulnerability resulting from climate change. These

three existing taxonomic grades are suitable for all field crops. With the need to pay attention to nitrogenous, phosphorous, and potassium fertilization to maintain soil stocks, and the need to update plants' water needs.

#### 4. Conclusions

The research was able to categorize the areas that are highly sensitive to climate change and the reasons behind the sensitivity. It was essential to target the correct cause that is leading to the depletion of the fertile land in Egypt's Nile Delta which will more likely leads to desertification of the region over time. Land degradation that will lead to desertification can impact the local population's health and food security in Egypt. In order to accomplish SDG 15.3, the government must make the recognized areas of land degradation in this document the primary targets of restoration efforts, particularly in the Nile Delta region. Additionally, land degradation is the result of anthropogenic driving factors as well as SLR. Future research, by the authors, proposes using the ESI on the district level to gauge the socio-economic influences of land degradation on the wealth of individuals in Egypt's Nile Delta and the extent to which land degradation has impacted agriculture revenues and impacted the labour force there. By that, poverty targeting plans coupled with crop suitability and monitoring may slow down land degradation in one of the world's most climate-risk areas and where many of the world's poor remain vulnerable.

#### Conflicts of interest

There is no dispute or disagreement over this research.

**Formatting of funding sources:** This research was not funded by any organization.

**Acknowledgments:** The authors are grateful to the Agricultural Research Center (ARC), Egypt's Soils, Water & Environment Research Institute for their technical assistance.

#### 5. References

- Abdullahi, M. B., Elnaggar, A. A., Omar, M. M., Murtala, A., Lawal, M. & Mosa, A. (2023). LAND DEGRADATION, CAUSES, IMPLICATIONS AND SUSTAINABLE MANAGEMENT IN ARID AND SEMI ARID REGIONS: A CASE STUDY OF EGYPT. *Egypt. J. Soil Sci.* 63(4). [https://ejss.journals.ekb.eg/article\\_319383.html](https://ejss.journals.ekb.eg/article_319383.html)
- Afzali, S. F., Khanamani, A., Maskooni, E. K., & Berndtsson, R. (2021). Quantitative assessment of environmental sensitivity to desertification using the modified MEDALUS model in a semiarid area. *Sustainability*, 13(14), 7817. <https://doi.org/10.3390/su13147817>.
- Ait Lamqadem, A., Pradhan, B., Saber, H., & Rahimi, A. (2018). Desertification Sensitivity Analysis Using MEDALUS Model and GIS: A Case Study of the Oases of Middle Draa Valley, Morocco. *Sensors*, 18(7), 2230. doi: <https://doi.org/10.3390/s18072230>.

- Arnoldus, H. M. J. (1977). Methodology used to determine the maximum potential average annual soil loss due to sheet and rill erosion in Morocco. *FAO Soils Bulletins*, *FAO*.
- Bedoui, C. (2020). Study of desertification sensitivity in Talh region (Central Tunisia) using remote sensing, G.I.S. and the M.E.D.A.L.U.S. approach. *Geoenvironmental Disasters*, *7*(1), 16. doi: <https://doi.org/10.1186/s40677-020-00148-w>
- Bontemps, S., Defourny, P., Brockmann, C., Herold, M., Kalogirou, V., & Arino, O. (2012). New global land cover mapping exercise in the framework of the ESA Climate Change Initiative. *IEEE International Geoscience and Remote Sensing Symposium*. 2012, 44–47. <https://doi.org/10.1109/igarss.2012.6351640>.
- Boudjemline, F., & Semar, A. (2018). Assessment and mapping of desertification sensitivity with MEDALUS model and GIS—Case study: basin of Hodna, Algeria. *Journal of Water and Land Development*, *36* (I–III), 17–26. doi: <https://doi.org/10.2478/jwld-2018-0002>
- Budak, M., Günal, H., Çelik, İ., Yıldız, H., Acir, N., & Acar, M. (2018). Environmental sensitivity to desertification in northern Mesopotamia; application of modified MEDALUS by using analytical hierarchy process. *Arabian Journal of Geosciences*, *11*(17), 481. doi: <https://doi.org/10.1007/s12517-018-3813-y>
- CAPMAS, (2022). Central Agency for Public Mobilization and Statistics, Statistical Data Dissemination Policy, 75, January 2022. <https://www.capmas.gov.eg>
- CIESIN, (2018). Gridded Population of the World, Version 4 (GPWv4): Population Density, Revision 11. NASA Socioeconomic Data and Applications Center (SEDAC). Center for International Earth Science Information Network - CIESIN - Columbia University, Palisades, NY <https://doi.org/10.7927/H49C6VHW>.
- De Pina Tavares, J., Baptista, I., Ferreira, A. J. D., Amiotte-Suchet, P., Coelho, C., Gomes, S., Amoros, R., Dos Reis, E. A., Mendes, A. F., Costa, L., Bentub, J., & Varela, L. (2015). Assessment and mapping the sensitive areas to desertification in an insular sahelian mountain region case study of the Ribeira Seca watershed, Santiago Island, Cabo Verde. *CATENA*, *128*, 214–223. <https://doi.org/10.1016/j.catena.2014.10.005>.
- Elbasiouny, H. (2018). Assessment of Environmental Sensitivity to Desertification, Soil Quality and Sustainability in An Area of The North Nile Delta, Egypt. *Egypt. Soil. Sci.* *58* (4), 399-415. [https://ejss.journals.ekb.eg/article\\_21553.html](https://ejss.journals.ekb.eg/article_21553.html)
- Elnashar, A., Wang, L., Wu, B., Zhu, W., & Zeng, H. (2021a). Synthesis of global actual evapotranspiration from 1982 to 2019. *Earth Syst. Sci. Data* *13*(2), 447–480. <https://doi.org/10.5194/essd-13-447-2021>
- Elnashar, A., Zeng, H., Wu, B., Fenta, A.A., Nabil, M. & Duerler, R. (2021b). Soil erosion assessment in the Blue Nile Basin driven by a novel RUSLE-GEE framework. *Sci. Total Environ.* *793*, 148466. <https://doi.org/10.1016/j.scitotenv.2021.148466>
- Elnashar, A., Zeng, H., Wu, B., Gebremicael, T. G., & Marie, Kh. (2022). Assessment of environmentally sensitive areas to desertification in the Blue Nile Basin driven by the MEDALUS-GEE framework. *Sci. Total Environ.* *815*, 152925. <http://dx.doi.org/10.1016/j.scitotenv.2022.152925>
- ESA, (2015). Land Cover CCI Product User Guide Version 2.0. Available at: <http://maps.elie.ucl.ac.be/CCI/viewer/download.php>. (Accessed 7 October 2018) European Space Agency.
- ESA, (2018). Land Cover CCI Product User Guide Version 2.0.7. Available at: <http://maps.elie.ucl.ac.be/CCI/viewer/download.php>. (Accessed 7 October 2018) European Space Agency.
- Fenta, A. A., Tsunekawa, A., Haregeweyn, N., Tsubo, M., Yasuda, H., Kawai, T., Ebabu, K., Berihun, M. L., Belay, A. S., & Sultan, D. (2021). Agroecology-based soil erosion assessment for better conservation planning in Ethiopian River basins. *Environmental Research*, *195*, 110786. <https://doi.org/10.1016/j.envres.2021.110786>.
- Ferrara, A., Kosmas, C., Salvati, L., Padula, A., Mancino, G., & Nolè, A. (2020). Updating the MEDALUS-ESA framework for Worldwide Land Degradation and desertification assessment. *Land Degradation & Development*, *31*(12), 1593–1607. <https://doi.org/10.1002/ldr.3559>.
- Funk, C., Peterson, P., Landsfeld, M., Pedreros, D., Verdin, J., Shukla, S., Husak, G., Rowland, J., Harrison, L., Hoell, A., & Michaelsen, J. (2015). The climate hazards infrared precipitation with stations—a new environmental record for monitoring extremes. *Scientific Data*, *2*(1). <https://doi.org/10.1038/sdata.2015.66>.
- Giuliani, G., Mazzetti, P., Santoro, M., Nativi, S., Van Bemmelen, J., Colangeli, G., & Lehmann, A. (2020). Knowledge generation using satellite Earth observations to support Sustainable Development Goals (SDG): A use case on land degradation. *International Journal of Applied Earth Observation and Geoinformation*, *88*, 102068. <https://doi.org/10.1016/j.jag.2020.102068>.
- Gorelick, N., Hancher, M., Dixon, M., Ilyushchenko, S., Thau, D. & Moore, R., (2017). Google earth engine: planetary-scale geospatial analysis for everyone. *Remote Sens. Environ.* *202*, 18–27.
- Hartmann, J., & Moosdorf, N. (2012). The new global lithological map database GLiM: A representation of rock properties at the Earth surface. *Geochemistry, Geophysics, Geosystems*, *13*(12).
- Hengl, T., Mendes de Jesus, J., Heuvelink, G. B., Ruiperez Gonzalez, M., Kilibarda, M., Blagotić, A., & Kempen, B. (2017). SoilGrids250m: Global gridded soil information based on machine learning. *PLoS one*, *12*(2), e0169748.
- Jafari, R., & Bakhsh and Ehmehr, L. (2016). Quantitative Mapping and Assessment of Environmentally Sensitive Areas to Desertification in Central Iran. *Land Degradation & Development*, *27*(2), 108-119. doi: <https://doi.org/10.1002/ldr.2227>
- IPCC, (2022). Adaptation, and Vulnerability Contribution of Working Group II to the Sixth Assessment Report of the Intergovernmental Panel on Climate Change [H.-O. Pörtner, D.C. Roberts, M. Tignor, E.S. Poloczanska, K. Mintenbeck, A. Alegría, M. Craig, S. Langsdorf, S. Löschke, V. Möller, A. Okem, & B. Rama (eds.)]. Cambridge University Press. Cambridge University Press, Cambridge, UK and New York, NY, USA, 3056 pp., doi:10.1017/9781009325844.
- Jarvis, A., Reuter, H. I., Nelson, A., & Guevara, E. (2008). Hole-filled SRTM for the globe Version 4. available from the CGIAR-CSI SRTM 90m Database <http://srtm.csi.cgiar.org>, 15(25-54), 5.
- Kamal, A., Sarah, R., Nicholas, S. P., Alex, de S., Jane, L., Chris, H., Bryan, J., et al. (2023). African Shifts:

- The Africa Climate Mobility Report, Addressing Climate-Forced Migration & Displacement; Africa Climate Mobility Initiative and Global Centre for Climate Mobility, New York. © Global Centre for Climate Mobility, <https://africa.climate-mobility.org/report>, License: CC BY-NC 4.0
- Kosmas, C., Kairis, O., Karavitis, C., Ritsema, C., Salvati, L., Acikalin, S., & Ziogas, A. (2014). Evaluation and Selection of Indicators for Land Degradation and Desertification Monitoring: Methodological Approach. *Environmental Management*, 54(5), 951-970. <https://doi.org/10.1007/s00267-013-0109-6>
- Kulp, S.A., & Strauss, B. H. (2019). New elevation data triple estimates of global vulnerability to sea-level rise and coastal flooding. *Nat Commun* 10, 4844 (2019). <https://doi.org/10.1038/s41467-019-12808-z>
- Lahlaoui, H., Rhinane, H., Hilali, A., Lahssini, S., & Moukrim, S. (2017). Desertification assessment using medalus model in watershed Oued El Maleh, Morocco. *Geosciences*, 7(3), 50. <https://doi.org/10.3390/geosciences7030050>.
- McNamara, I., Baez-Villanueva, O. M., Zomorodian, A., Ayyad, S., Zambrano-Bigiarini, M., Zaroug, M., Mersha, A., Nauditt, A., Mbuliro, M., Wamala, S., & Ribbe, L. (2021). How well do gridded precipitation and actual evapotranspiration products represent the key water balance components in the Nile Basin? *Journal of Hydrology: Regional Studies*, 37, 100884. <https://doi.org/10.1016/j.ejrh.2021.100884>.
- Moghanm, F. S. and Belal, A. B. (2018). Assessment and Mapping of Environmentally Sensitive Areas To Desertification Using Gis in An Area of The North Delta Region of Egypt. *Egypt. J. Soil Sci.* 58 (3), 325-335. [https://ejss.journals.ekb.eg/article\\_13488.html](https://ejss.journals.ekb.eg/article_13488.html)
- Momirović, N., Kadović, R., Perović, V., Marjanović, M., & Baumgertel, A. (2019). Spatial assessment of the areas sensitive to degradation in the rural area of the municipality čukarica. *International Soil and Water Conservation Research*, 7(1), 71–80. <https://doi.org/10.1016/j.iswcr.2018.12.004>.
- Morianou, G., Kourgiyalas, N. N., Pisinaras, V., Psarras, G., & Arambatzis, G. (2021). Assessing desertification sensitivity map under climate change and agricultural practices scenarios: The island of crete case study. *Water Supply*, 21(6), 2916–2934. <https://doi.org/10.2166/ws.2021.132>.
- Nada, W. M., Abou Hussien, El. & Elbaalawy, A. M. (2023). Biochemical Properties of Calcareous Soil Affected by the Source of Sulphur-Organic Fertilizers. *Egypt. J. Soil Sci.* 63( 2), 255-265. [https://ejss.journals.ekb.eg/article\\_298672.html](https://ejss.journals.ekb.eg/article_298672.html)
- Právělie, R., Patriche, C., Bandoc, G., (2017). Quantification of land degradation sensitivity areas in southern and central southeastern Europe. new results based on improving DISMED methodology with new climate data. *Catena* 158, 309–320.
- Saleh, A. M. Belal, A. B. & Jalhoum, M. E. (2018). Quantitative Assessment of Environmental Sensitivity to Desertification in Sidi Abdel-Rahman Area, Northern West Coast of Egypt. *Egypt. J. Soil Sci.* 58 (1), 13 -26. [https://ejss.journals.ekb.eg/article\\_4057.html](https://ejss.journals.ekb.eg/article_4057.html)
- Sdiri, A., Pinho, J., Ratanatamskul, C., (2018). Water resource management for sustainable development. *Arab. J. Geosci.* 11, 124.
- Senay, G. B., Bohms, S., Singh, R. K., Gowda, P. H., Velpuri, N. M., Alemu, H., & Verdin, J. P. (2013). Operational evapotranspiration mapping using remote sensing and weather datasets: A new parameterization for the SSEB approach. *JAWRA Journal of the American Water Resources Association*, 49(3), 577–591. <https://doi.org/10.1111/jawr.12057>.
- Sepehr, A., Hassanli, A. M., Ekhtesasi, M. R., & Jamali, J. B. (2007). Quantitative assessment of desertification in south of Iran using MEDALUS method. *Environmental Monitoring and Assessment*, 134(1), 243. doi: <https://doi.org/10.1007/s10661-007-9613-6>
- Symeonakis, E., & Drake, N. (2004). Monitoring desertification and land degradation over sub-Saharan Africa. *International Journal of Remote Sensing*, 25(3), 573-592. doi: <https://doi.org/10.1080/0143116031000095998>
- Shukla, P., Skeg, J., Buendia, E.C., Masson-Delmotte, V., Portner, H.-O., & Roberts, D., (2019). Climate Change and Land: An IPCC Special Report on Climate Change, Desertification, Land Degradation, Sustainable Land Management, Food Security, and Greenhouse Gas Fluxes in Terrestrial Ecosystems.
- Trabucco, A., & Zomer, R. J. (2018). Global aridity index and potential evapotranspiration (ET0) climate database v2. CGIAR Consort Spat Inf, 10, m9.
- UNCCD, (2017). United Nations Convention to Combat Desertification - Global Land Outlook UNCCD Secretariat, Bonn, Germany.
- Van Velthuisen, H. (2007). Mapping biophysical factors that influence agricultural production and rural vulnerability: Food and Agriculture Organization of the United Nations and the International Institute of Applied Systems Analysis, Rome, Italy.
- Vousdoulas, M.I., Clarke, J., Ranasinghe, R., Reimann, L., Khalaf, N., Duong, T. M., et al. (2022). African heritage sites threatened as sea-level rise accelerates. *Nat. Clim. Chang.* 12, 256–262. <https://doi.org/10.1038/s41558-022-01280-1>.
- Wang, W., Samat, A., Ge, Y., Ma, L., Tuheti, A., Zou, S., & Abuduwaili, J. (2020). Quantitative soil wind erosion potential mapping for Central Asia using the Google Earth Engine Platform. *Remote Sensing*, 12(20), 3430. <https://doi.org/10.3390/rs12203430>.
- Weststrate, J., Dijkstra, G., Eshuis, J., Gianoli, A., & Rusca, M., (2019). The sustainable development goal on water and sanitation: learning from the millennium development goals. *Soc. Indic. Res.* 143, 795–810.
- Wijitkosum, S. (2021). Factor influencing land degradation sensitivity and desertification in a drought prone watershed in Thailand. *International Soil and Water Conservation Research*, 9(2), 217–228. <https://doi.org/10.1016/j.iswcr.2020.10.005>.
- Zhang, Y., Kong, D., Gan, R., Chew, F. H. S., McVicar, T. R., Zhang, Q., & Yang, Y. (2019). Coupled estimation of 500 m and 8-day resolution global evapotranspiration and Gross Primary Production in 2002–2017. *Remote Sensing of Environment*, 222, 165–182. <https://doi.org/10.1016/j.rse.2018.12.031>.